Liquid Crystals
Publication details, including instructions for authors and subscription information:
http://www.informaworld.com/smpp/title~content=t713926090

Numerical analysis for a nematic droplet in polymer dispersed liquid crystals

T. Onozawa[a]
[a] Development Department (22-28441), Color LCD Division, NEC Corporation, Kawasaki, Kanagawa, Japan

To cite this Article Onozawa, T.(1994) 'Numerical analysis for a nematic droplet in polymer dispersed liquid crystals', Liquid Crystals, 17: 5, 635 — 649
To link to this Article: DOI: 10.1080/02678299408037335
URL: http://dx.doi.org/10.1080/02678299408037335

LIQUID CRYSTALS, 1994, VOL. 17, NO. 5, 635–649

Numerical analysis for a nematic droplet in polymer dispersed liquid crystals

by T. ONOZAWA

Development Department (22-28441), Color LCD Division, NEC Corporation, 1753 Shimonumabe, Nakaharaku, Kawasaki, Kanagawa, 211, Japan

(Received 10 March 1994; acepted 25 March 1994)

Starting from the Landau-de Gennes free energy expression, the author has numerically analysed the director pattern in a nematic droplet of polymer dispersed liquid crystals. The nematic director has been understood as the eigenvector, which corresponds to the largest eigenvalue of the tensor order parameter. To investigate the droplet structure influence, all equations have been treated on the curvilinear coordinate system which is generated along the droplet boundary. In the case of spherical and spheroidal droplets with normal strong anchoring, the director exhibits an axial configuration and a disclination ring. The ring radius and the capactiance of the system change without hysteresis with the applied voltage.

1. Introduction

A polymer dispersed liquid crystal display (PDLCD) [1] is now very interesting, because it is expected to offer a wide viewing angle and high brightness [2]. Its operational mode is based on the control of light scattering by applied voltage. At zero or low field, directors orient axially or radially in a cavity [3], if an alignment on the cavity surface is normal. Therefore, differences in refractive index between the droplet and the surrounding material become large and light waves are strongly scattered by the droplets. On the contrary, directors in cavities line up almost parallel to the applied electric field direction at higher applied voltages and the difference is lost. Then, the PDLCD becomes transparent.

However, detailed analyses have not yet been accomplished for the director behaviour in the droplet, when, at least, voltages are applied to the PDLCD. Moreover, it is well known that PDLCD exhibits hysteresis in its electro-optical characteristics, when an applied voltage is changed from lower to higher values and vice versa. The electro-optical properties of the PDLCD, including the hysteresis, depend strongly upon the droplet size, droplet structure, and structure distribution, as well as material parameters, such as elastic constants of the nematic liquid crystal and dielectric permittivity of both the liquid crystal and polymer.

In this paper, the author has numerically investigated the behaviour of directors in a PDLCD by solving simultaneously the Euler-Lagrange equation for the tensor order parameter obtained from the Landau-de Gennes free energy [4] and the generalized Poisson equation, when an electric field is applied to PDLCD. In order to investigate the structure effects mentioned above, all equations have been treated on the curvilinear coordinate system, which is generated along nematic droplet boundaries [5]. Therefore, the simulation program used is applicable for an arbitrary

*Author for correspondence.

0267–8292/94 $10·00

shape of a nematic droplet. It has been assumed, for simplicity, that the problem is solved in two-dimensional space; however directors can deform only in a plane. From symmetry consideration, the treatment can be applied for a droplet having a rotational symmetry, such as a sphere or spheroids.

Optical scattering power is very difficult to calculate from the director pattern in a droplet [6–8]. Therefore, the differential electric capacitance of the PDLCD has been studied as a system response to the external fields.

For a spherical droplet and a spheroidal droplet with a normal strong anchoring alignment on its surface, the director pattern becomes axial and involves a discliniation ring. The author has assumed that the director is given as the eigenvector corresponding to the largest eigenvalue of the tensor order parameter, because the tensor order parameter, not the director, has been obtained form the Euler-Lagrange equation. The disclination ring radius changes uniquely with a change in an applied voltage and the electric capacity does not show any hysteresis with respect to an applied voltage.

However, if the same problem is solved by using the Kilian and Hess method [9, 10] as shown in Appendix B, a large hysteresis appeared in director distribution and electric capacity. The hysteresis origin is considered to be the nonlinearity involves in Kilian and Hess's method.

The next section describes the numerical procedures on the curvilinear coordinate system and illustrates how to derive the nematic director. The third section presents some numerical results which have been obtained for one droplet in the PDLCD. A summary and conclusion are given in the last section.

2. Mathematical procedures

Nematic liquid crystals are characterized by a traceless symmetric tensor order parameter S_{ij} in describing their elastic properties. By using this tensor order parameter, the Landau-de Gennes free energy density is given, under one constant approximation, as

$$g_s=\frac{1}{2}L_1(\partial_i S_{jk})(\partial_i S_{jk})-\frac{1}{2}\varepsilon_a E_i E_j S_{ij} \tag{1}$$

in the cartesian coordinate. In equation (1), the summation convention is adopted. It was assumed that the scalar order parameter in tensor order parameter was constant. ε_a is an anisotropic dielectric permittivity of a nematic liquid crystal and E_i represents an applied electric field component.

The Euler-Lagrange equations are derived from equation (1) by differentiation with respect to S_{ij}, which accompany $\mathrm{Tr}(S_{ij})=0$ and $S_{ij}=S_{ji}$ as subsidiary conditions.

$$\Delta S_{ij}+\frac{1}{2}\varepsilon_a E_i E_j=\Lambda_{ij}, \tag{2}$$

where Λ_{ij} is the Lagrange parameter tensor [11].

$$\Lambda_{ij}=\lambda_0\delta_{ij}-\varepsilon_{ijk}\lambda_k. \tag{3}$$

ε_{ijk} implies the complete antisymmetric tensor of rank 3. It should be noticed that equation (2) is a linear partial differential equation with respect to the tensor order parameter S_{ij}.

An electric field is given by solving the generalized Poisson equation

$$\nabla_i(\varepsilon_{ij}E_j) = -\nabla_i(\varepsilon_{ij}\nabla_j V) = 0. \tag{4}$$

Here, the dielectric permittivity tensor ε_{ij} has the relation with the nematic director

$$\varepsilon_{ij} = \varepsilon_\perp \delta_{ij} + \varepsilon_a n_i n_j. \tag{5}$$

However, these treatments on the Cartesian coordinate system are very inconventient, when objects being analysed have a complex boundary structure. Therefore, in order to avoid this inconvenience, a curvilinear coordinate system is utilized. In the following, a two-dimensional problem is treated for simplicity and the director is confined to have components only in the plane.

The discretization lattice is formed in the way illustrated in Appendix A. It is essential that the lattice lines constitute the curvilinear coordinate line ξ^i. The covariant base vector $\mathbf{e}_i$ is defined at each lattice point, as shown in figure 1. $\mathbf{e}_i$ are not unit vectors and are not mutually perpendicular. To complement the non-orthogonality of the covariant base vectors, the contravariant base vector $\mathbf{e}^i$ is given as

$$\mathbf{e}^i = \frac{\mathbf{e}_j \times \mathbf{e}_k}{\mathbf{e}_i \cdot (\mathbf{e}_j \times \mathbf{e}_k)} \qquad (i, j, k \text{ cyclic}). \tag{6}$$

If we denote the base vectors as $(\mathbf{i}, \mathbf{j}, \mathbf{k}) = (\mathbf{e}_{01}, \mathbf{e}_{02}, \mathbf{e}_{03}) = (\mathbf{e}_0^1, \mathbf{e}_0^2, \mathbf{e}_0^3)$ in the cartesian coordinate system, $\mathbf{e}_i$ are given as

$$\mathbf{e}_1 = \mathbf{i}x_\xi + \mathbf{j}y_\xi, \qquad \mathbf{e}_2 = \mathbf{i}x_\eta + \mathbf{j}y_\eta, \qquad \text{and} \qquad \mathbf{e}_3 = \mathbf{k}. \tag{7}$$

Here, x_ξ etc., mean the derivative of x by the curvilinear coordinate ξ. Equation (7) is rewritten

$$\mathbf{e}_i = \bar{A}_i^j \mathbf{e}_{0j}. \tag{8}$$

Matrix $\bar{A}_j^i$ is known from equation (7)

$$(\bar{A}_j^i) = \left(\frac{\partial x^i}{\partial \xi^j}\right) = \begin{bmatrix} x_\xi & x_\eta & 0 \\ y_\xi & y_\eta & 0 \\ 0 & 0 & 1 \end{bmatrix}. \tag{9}$$

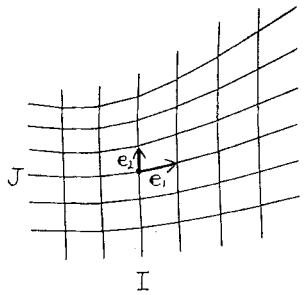

Figure 1. Covariant base vectors are defined at each lattice point. $\mathbf{e}_1$ is the vector directing from lattice point (I, J) to $(I+1, J)$. $\mathbf{e}_2$ is the vector directing from lattice point (I, J) to $(I, J+1)$. These vectors are not of unit length and are not mutually orthogonal.

The contravariant base vectors are given by a matrix A_j^i, which is the inverse matrix of $\bar{A}_j^i$.

$$\mathbf{e}^i = A_j^i \mathbf{e}_0^j. \tag{10}$$

$$A_k^i \bar{A}_j^k = \bar{A}_k^i A_j^k = \delta_j^i. \tag{11}$$

The covariant and contravariant metric tensor components are derived in the same way, which are necessary in the later calculations. From $g_{ij} = \mathbf{e}_i \cdot \mathbf{e}_j$ for the covariant metric tensor, we obtain

$$\left.\begin{aligned} g_{11} &= (x_\xi)^2 + (y_\xi)^2, \\ g_{22} &= (x_\eta)^2 + (y_\eta)^2, \\ g_{33} &= 1, \\ g_{12} &= g_{21} = x_\xi x_\eta + y_\xi y_\eta, \\ g_{13} &= g_{31} = g_{23} = g_{32} = 0, \\ J &= \sqrt{(g_{11} g_{22} - g_{12}{}^2)}. \end{aligned}\right\} \tag{12}$$

Here, J is the jacobian function of the transformation. The contravariant metric tensor g^{ij} is easily obtained from the relation

$$g^{ik} g_{kj} = \delta_j^i. \tag{13}$$

A director of nematic liquid, which is a unit vector, is described in various forms, according to the base vectors. If we denote it as $\mathbf{n}$, then

$$\mathbf{n} = n_0^i \mathbf{e}_{0i} = n_{0i} \mathbf{e}_0^i = n^i \mathbf{e}_i = n_i \mathbf{e}^i. \tag{14}$$

It should be noticed that the covariant and contravariant components are not different in the cartesian coordinate. The relations between individual nomenclatures are readily determined from the transformation rule for the base vector. In the curvilinear coordinate, covariant components are obtained as

$$n_i = \bar{A}_i^j n_{0j}. \tag{15}$$

The contravariant components are obtained as

$$n^i = A_j^i n_0^j. \tag{16}$$

For the tensor order parameter, the symmetric contravariant components are obtained from the director components, which are defined above.

$$S^{ij} = S\left(n^i n^j - \frac{1}{3} g^{ij}\right). \tag{17}$$

The mixed tensor order parameter is

$$S_j^i = S\left(n^i n_j - \frac{1}{3} \delta_j^i\right). \tag{18}$$

This expression is utilized to show that the tensor order parameter is traceless.

The partial differential equation (2) for the tensor order parameter is converted to the one corresponding to the curvilinear coordinate system, if we replace a usual derivative with a covariant derivative.

$$\Delta S^{ij}+\frac{1}{2}\varepsilon_a E^i E^j=\nabla^k(\nabla_k S^{ij})+\frac{1}{2}\varepsilon_a E^i E^j=\Lambda^{ij} \tag{19}$$

and for the mixed components,

$$\nabla^k(\nabla_k S^i_j)+\frac{1}{2}\varepsilon_a E^i E_j=\Lambda^i_j. \tag{20}$$

A covariant derivative for the tensor is given as

$$\nabla_k S^{ij}=\partial_k S^{ij}+\Gamma^i_{km}S^{mj}+\Gamma^j_{km}S^{im}, \tag{21}$$

and

$$\nabla_k S^i_j=\partial_k S^i_j+\Gamma^i_{km}S^m_j-\Gamma^m_{kj}S^i_m. \tag{22}$$

These constitute tensors of rank 3. Here, Γ^i_{jk} represents Christoffel's symbol and is defined as

$$\Gamma^i_{jk}=\frac{1}{2}g^{im}\left(\frac{\partial g_{mj}}{\partial \xi^k}+\frac{\partial g_{mk}}{\partial \xi^j}-\frac{\partial g_{jk}}{\partial \xi^m}\right) \tag{23}$$

where Γ^1_{11}, Γ^1_{12}, Γ^1_{21}, Γ^1_{22}, Γ^2_{11}, Γ^2_{12}, Γ^2_{21} and Γ^2_{22} are non-zero in Γ^i_{jk}, when metric tensor components are given as equations (12) and (13) in the two-dimensional case.

From the symmetry property of equation (19), λ_k of the Lagrange tensor is obtained and λ_0 is given by taking trace of equation (20). If we eliminate the Lagrange parameter tensor from expression (19), we obtain the equation to be solved for the contravariant components,

$$\nabla^k(\nabla_k S^{ij})+\frac{1}{2}\varepsilon_a\overline{E^iE^j}=g^{km}\nabla_m(\nabla_k S^{ij})+\frac{1}{2}\varepsilon_a\overline{E^iE^j}=0 \tag{24}$$

where

$$\overline{E^iE^j}=\left(E^iE^j-\frac{1}{3}g^{ij}|E|^2\right). \tag{25}$$

Equation (24) includes the covariant derivative of a mixed tensor of rank 3.

The generalized Poisson equation (4) is transformed onto the curvilinear coordinate system at the same time:

$$\nabla_i(\varepsilon^i_j E^j)=-\nabla_i(\varepsilon^i_j\nabla^j V)=0. \tag{26}$$

The dielectric permittivity tensor ε^i_j relates to the liquid crystal director

$$\varepsilon^i_j=\varepsilon_\perp\delta^i_j+\varepsilon_a n^i n_j. \tag{27}$$

Two-coupled partial differential equations, equations (24) and (26), should be solved simultaneously. However, the dielectric permittivity tensor ε^i_j is not given by the tensor order parameter but by the director of liquid crystal. Although ε^i_j is formally written by using S^i_j, the expression equation (27) is preferred. The reason is

that the director is a unit vector. If we use S^i_j in equation (27), then ε^i_j unlimitedly increases proportionally to an applied field strength, because $Tr(S^i_j)=0$ never restrict the magnitude of the tensor order parameter.

The director has been interpreted as the eigenvector [12], which corresponds to the largest eigenvalue of the characteristic equation of the symmetric tensor S^{ij}. Actually calculating the eigenvector is convenient on the Cartesian coordinate system. S^{ij} is inversely transformed to obtain S^{ij}_0. Then, the characteristic equation is

$$\begin{pmatrix} S_0^{11}-\mu & S_0^{12} \\ S_0^{12} & S_0^{22}-\mu \end{pmatrix}\begin{pmatrix} n_0^1 \\ n_0^2 \end{pmatrix}=0, \tag{28}$$

because we have assumed that $n^3_0=0$. For the eigenvector n^i_0, it is possible to impose the condition

$$(n_0^1)^2+(n_0^2)^2=1. \tag{29}$$

For the largest eigenvalue μ_0 of equation (28), the eigenvector is derived from equations (28) and (29)

$$n_0^1=\pm\sqrt{\left(\frac{(S_0^{22}-\mu_0)^2}{(S_0^{22}-\mu_0)^2+(S_0^{12})^2}\right)}, \tag{30a}$$

and

$$n_0^2=-\frac{S_0^{12}}{S_0^{22}-\mu_0}n_0^1. \tag{30b}$$

It is clear that a selection of $+/-$ sign in expression (30*a*) does not affect ε^i_j defined by equation (27). This means that the director is equivalent for both directions. The cartesian component n^i_0 is converted to the curvilinear component according to equations (15) and (16). Then, these are substituted into equation (27). If ε_a is set equal to zero and $\varepsilon_\perp$ is replaced by the dielectric permittivity of polymer in equation (26), the same equation can be used for the polymer.

For the boundary between nematic droplet and polymer, the vertical components of electric displacement vectors are equal on the both side of the droplet and the polymer.

$$D^i_{\text{droplet}}=D^i_{\text{polymer}} \tag{31}$$

and

$$\left.\begin{aligned} D^i_{\text{droplet}}&=\varepsilon^i_j E^j \quad \text{for the nematic droplet,} \\ D^i_{\text{polymer}}&=\varepsilon_0 E^i \quad \text{for the polymer.} \end{aligned}\right\} \tag{32}$$

(*b*)

Here, ε_0 is the dielectric permittivity of a polymer material.

Equations (24), (26), and (31) are discretized and numerically solved by the SOR method with appropriate boundary conditions. The author assumed, on discretizing, that the tensor order parameters are given at each lattice point and that the electric potential is given at the centre of the area surrounded by four lattice lines. The discretization of the term including S^{ij} in equation (24) is given, for example, as follows for the component $k=1$, $m=1$, $i=1$ and $j=1$ at the lattice point (I, J):

$$
\begin{aligned}
&g^{11}(I,J)\{\partial_1\partial_1 S^{11}+\partial_1(\Gamma^1_{1m}S^{m1}+\Gamma^1_{1m}S^{1m})-\Gamma^n_{11}(\partial_n S^{11}+\Gamma^1_{nm}S^{m1}+\Gamma^1_{nm}S^{1m})\\
&\quad+\Gamma^1_{1n}(\partial_1 S^{n1}+\Gamma^n_{1m}S^{m1}+\Gamma^1_{1m}S^{nm})+\Gamma^1_{1n}(\partial_1 S^{1n}+\Gamma^1_{1m}S^{mn}+\Gamma^n_{1m}S^{1m})\}\\
&=g^{11}(I,J)\{(S^{11}(I+1,J)-2\cdot S^{11}(I,J)+S^{11}(I-1,J))\\
&\quad+\frac{1}{2}(\Gamma^1_{1m}(I+1,J)S^{m1}(I+1,J)-\Gamma^1_{1m}(I-1,J)S^{m1}(I-1,J))\\
&\quad+\frac{1}{2}(\Gamma^1_{1m}(I+1,J)S^{1m}(I+1,J)-\Gamma^1_{1m}(I-1,J)S^{1m}(I-1,J))\\
&\quad-\frac{1}{2}(\Gamma^1_{11}(I,J)\cdot(S^{11}(I+1,J)-S^{11}(I-1,J))\\
&\quad+\Gamma^2_{11}(I,J)\cdot(S^{11}(I,J+1)-S^{11}(I,J-1))\\
&\quad-\Gamma^n_{11}(I,J)\cdot(\Gamma^1_{nm}(I,J)S^{m1}(I,J)+\Gamma^1_{nm}(I,J)S^{1m}(I,J))\\
&\quad+\frac{1}{2}\Gamma^1_{1n}(I,J)\cdot(S^{n1}(I+1,J)-S^{n1}(I-1,J))\\
&\quad+\Gamma^1_{1n}(I,J)\cdot(\Gamma^n_{1m}(I,J)S^{m1}(I,J)+\Gamma^1_{1m}(I,J)S^{nm}(I,J))\\
&\quad+\frac{1}{2}\Gamma^1_{1n}(I,J)\cdot(S^{1n}(I+1,J)-S^{1n}(I-1,J))\\
&\quad+\Gamma^1_{1n}(I,J)\cdot(\Gamma^1_{1m}(I,J)S^{mn}(I,J)+\Gamma^n_{1m}(I,J)S^{1m}(I,J))\},
\end{aligned}
\tag{33}
$$

where the discretized form of Christoffel's symbol Γ^1_{11}, for example, is

$$
\begin{aligned}
\Gamma^1_{11}=&\frac{1}{4}g^{11}(I,J)\cdot(g_{11}(I+1,J)-g_{11}(I-1,J))\\
&-\frac{1}{2}g^{12}(I,J)\cdot((g_{12}(I+1,J)-g_{12}(I-1,J))\\
&-\frac{1}{2}(g_{11}(I,J+1)-g_{11}(I,J-1))).
\end{aligned}
\tag{34}
$$

Because equation (33) involves a derivative of the Christoffel's symbol, careful treatment is necessary to avoid a virtual extra-force generation.

3. Numerical results

In this paper, the author studied the cases in which only one nematic droplet exists in a polymer material between two electrode plates. The parameters used in the calculation are shown in table 1. It has been assumed that the director alignment on the droplet surface is normal and has a strong anchoring property.

Table 1. Parameters used in calculation.

Elastic coefficient	L_1	5×10^{-7} dyne
Parallel permittivity	$\varepsilon_\parallel$	20
Perpendicular permittivity	$\varepsilon_\perp$	7
Permittivity of polymer	ε_0	5·5

Four types of droplet shapes have been investigated. First is a sphere (*a*). Second is a spheroid (*b*), with the major axis perpendicular to the electrode plane. Third is a spheroid (*c*) with a parallel axis. The last one is a body of revolution (*d*), which has a complex but rotationally symmetric boundary structure. This example shows that the author's numerical procedures admit various shapes of nematic droplets. Cross-sectional views of PDLCDs, including these droplets, are shown in figure 2.

3.1. *Sphere*

The director distribution in the sphere takes an axial configuration in the absence of an external field, in which a disclination ring has a small radius, as shown in figure 3 (*a*). The axis direction is determined by an initial setting of the director distribution and by a lattice system used in the calculation.

When an external field is applied, the director distribution changes its shape. The disclination ring increases its radius according to an applied field strength, to be stuck on the droplet surface at higher applied voltages. The rings axis direction always becomes parallel to the applied field. Figure 3 (*b*) shows the director distribution, when 10 V are applied between the electrodes.

The equi-potential surface is shown in figure 3 (*c*) for the same applied voltage. It can be seen that the electric field is repelled out from the nematic droplet, because the dielectric permittivity becomes larger than the value of the surrounding polymer due to the director behaviour. Therefore, the coupling between equations (24) and (26) seems to be satisfactory.

3.2. *Spheroid with a perpendicular major axis*

Figure 4 (*a*) shows the director distribution at zero voltage in a spheroid which has a major principal axis perpendicular to the electrodes. In a spheroid, the disclination ring becomes an ellipse, whose major axis is coincident to that of the spheroid. Most directors align parallel to one minor principal axis for the spheroid in its central part. The reason is considered as being that the directors in this portion are more strongly affected by the side wall of the spheroid and align parallel to the director direction on the wall.

However, the alignment direction superiority is lost, when an electric field is applied. As can be seen in figure 4 (*b*), the directors readily align parallel to the

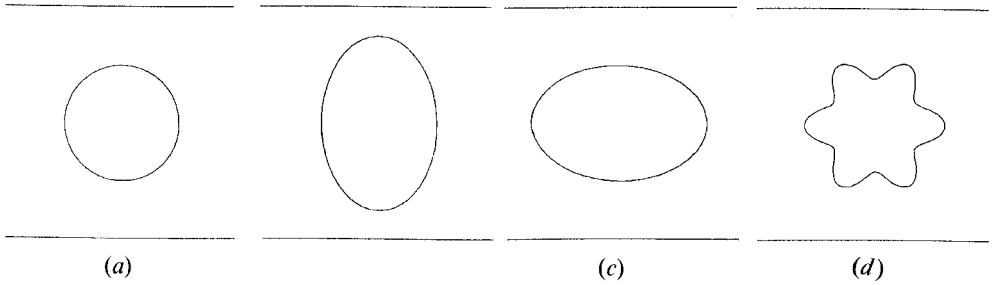

Figure 2. Figures illustrate the PDLCD cross-sections, which include one nematic droplet with rotational symmetry enclosed by a polymer material. The spacing between the electrodes is 5 μm. (*a*) 1·25 μm radius sphere. (*b*) spheroid whose major axis is perpendicular to the electrode surfaces and is 1·9 μm in length. The length of the minor axis is 1·25 μm. (*c*) spheroid whose major axis is parallel to the electrode surface. Major and minor axis lengths are the same as (*b*). (*d*) body of revolution in which a cusp height is 0·5 μm.

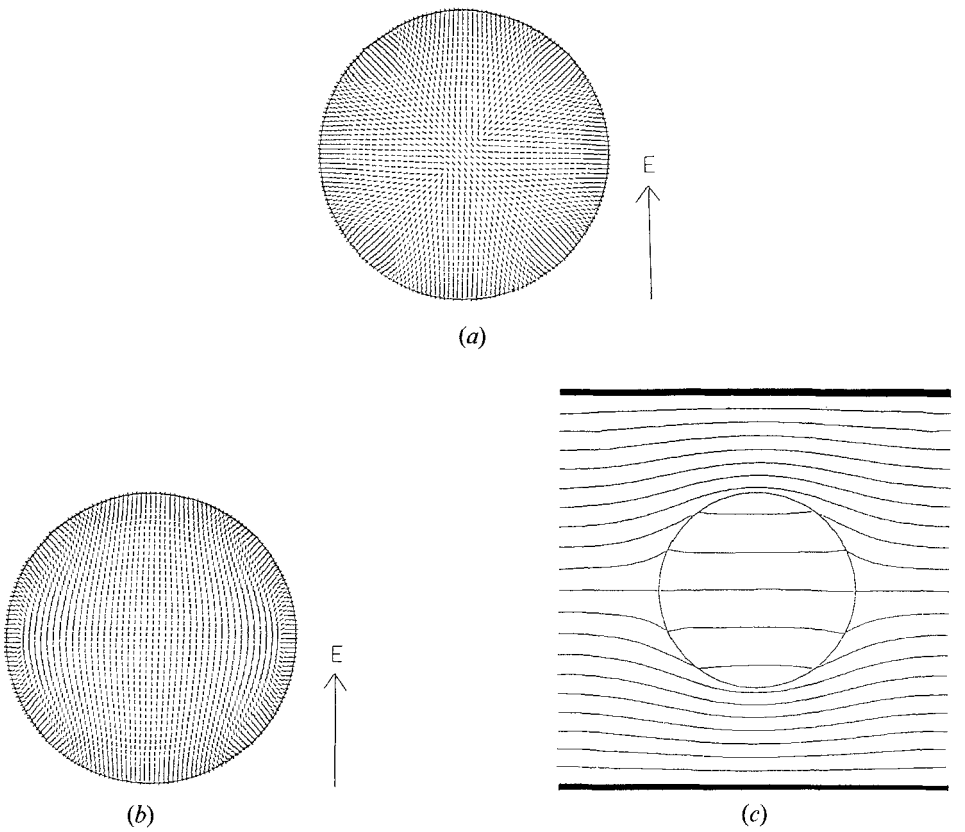

Figure 3. (*a*) Director distributes axially in the sphere in the absence of an external field. This distribution is retrieved after a high voltage application, if an applied voltage is set back to zero. (*b*) The pattern corresponds to that for 10 V application between electrodes. (*c*) The equipotential surface in PDLCD on applying 10 V.

applied field direction and the disclination ring lays in the plane including the minor principal axis of spheroid. As a result, in this case, pattern changes become large in the nematic droplet. After the electric field is set back to zero, the same director pattern as in figure 4 (*a*) reappears.

In this treatment, the totality of deformation energy over the disclination loop could not be obtained, because the procedure is essentially two dimensional. Therefore, it would be probable that the wall alignment effect is overestimated compared with the disclination energy.

3.3. *Spheroid with a parallel major axis*

For this droplet configuration at zero field, the director distribution is obtained by rotating the droplet, shown in figure 4 (*a*), by $\pi/2$. Therefore, it seems to be clear, from figure 5 (*a*), that most directors already align parallel to the applied electric field, although no field exists at zero applied voltage. An applied electric field expands the disclination ring and the perpendicular alignment region. In figure 5 (*b*), the pattern at 5 V is shown. It can be seen that a difference is small, compared with that for zero field.

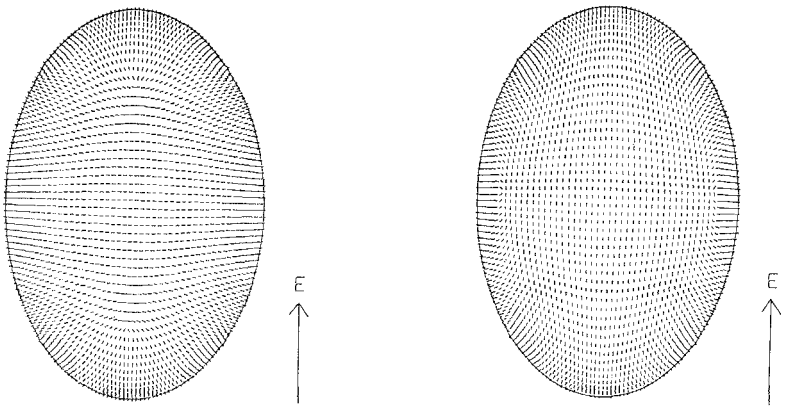

(*a*) (*b*)

Figure 4. Director configuration (*a*) in the absence of an external field, and (*b*) when 5 V are applied for the spheroidal droplet with perpendicular major axis.

3.4. *Electric capacity*

To investigate a response of PDLCD to an external field, a differential electric capacity

$$C(V)=\frac{\partial Q(V)}{\partial V}, \tag{35}$$

has been calculated for the capacitors including a nematic droplet illustrated in the above subsections. Here, $Q(V)$ is the electric charge stored on the electrode and obtained form the relation

$$Q(V)=-e\int\rho dv=\int\mathbf{div}\,\mathbf{D}\,dv=\int\mathbf{D}\,ds. \tag{36}$$

The surface integral in equation (36) is carried out on the electrode surface.

Figure 6 shows the differential capacities for PDLCDs including a droplet whose shape and director distribution have already been explained. In figure 6, the relative values are plotted to investigate the droplet shape effect. It can be seen that

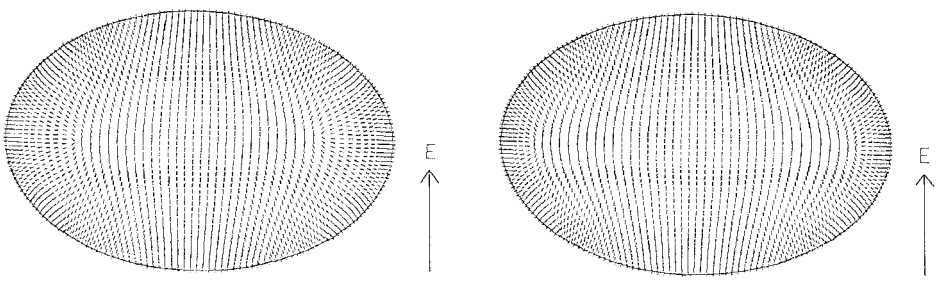

(*a*) (*b*)

Figure 5. Director configuration (*a*) in the absence of an external field, and (*b*) when 5 V are applied for the spheroidal droplet with parallel major axis.

individual capacity ratios are most different at zero voltage, but become almost equal at higher voltages. This electric capacity behaviour is well understood in consistent with the director distribution dependence on the droplet shape and an applied voltage.

No hysteresis exists in the capacity–voltage characteristic curves for all cases, even if a voltage is applied to a much higher value and is changed by a much larger step. Therefore, the author thinks that the hysteresis in the actual PDLCDs is brought about by other causes, such as a weak anchoring, a coupling between nematic droplets, or an electric polarization, etc.

However, if the same objects are treated by Kilian and Hess's method, the resultant differential capacity exhibits a large hysteresis, as described in Appendix B. It is supposed that the origin is the nonlinearity which exists in their equations for the director.

3.5. *Body of revolution*

One of the features of the author's treatment is that a droplet of more complex boundary is successfully analysed. As an example, the body of revolution, whose cross-section is shown in figure 2(*d*), has been studied. The director distribution in the body is shown in figure 7(*a*) for the zero applied voltage case.

Each convex part of the body includes a disclination line near its focal point. However, in the central part, the director distribution seems to be axial. On the boundary between the central part and convex part, another disclinations exist.

If an external field is applied, two disclination lines in both lateral convex parts remain, but others disappear, resulting in strong deformations in the director distribution in the droplet wall neighbourhoods. The situation is shown in figure 7(*b*).

4. Conclusions

By solving the linear Euler–Lagrage equations for a tensor order parameter in a curvilinear coordinate system, a numerical analysis, which is applicable to various

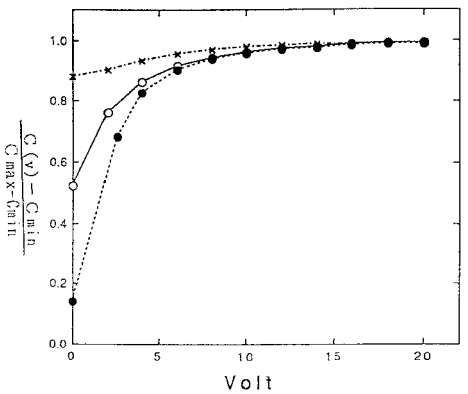

Figure 6. Differential electric capacity versus applied voltage characteristics. —○—, sphere; - - -●- - -, spheroid with perpendicular major axis; —— * - —, spheroid with parallel major axis. The electric capacity C_{min} is calculated for the director distribution in which all directors are set parallel to the electrode surface. The capacity C_{max} corresponds to perpendicular director distribution in the same way.

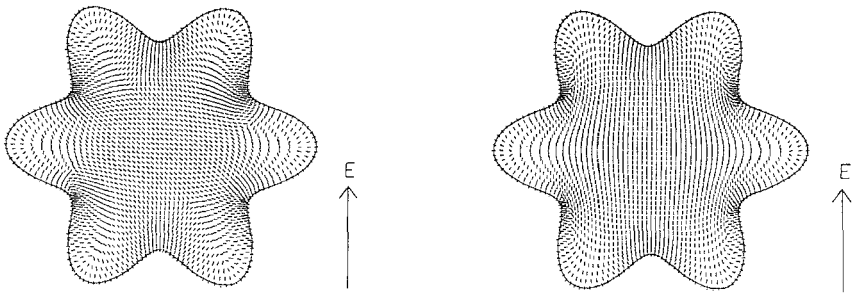

Figure 7. Director distribution (*a*) in the absence of an external field, and (*b*) when 5 V are applied for the droplet of body of revolution.

nematic droplet shapes, has been developed. The director distribution and electric capacity have been calculated for PDLCDs, which include nematic droplets with different cavity shapes.

The director has been interpreted as the eigenvector, which corresponds to the largest eigenvalue of the tensor order parameter. The director is used in the expression for the nematic dielectric permittivity tensor, because the tensor order parameter magnitude is not restricted by the property $\mathrm{Tr}\,(S_{\parallel}^{i})=0$.

No hysteresis has appeared in the director distribution and electric capacity dependences on an applied electric field, if one constant approximation is adopted. The author supposes that the hysteresis in the actual PDLCD is brought about by other origins, such as a weak anchoring, a coupling between nematic droplets, an electric polarization etc. It would be necessary to include these effects into the simulation model.

This work has been confined to the two-dimensional case, because the treatment becomes very complex and tedious in the three-dimensional curvilinear system, where metric tensor and Christoffel's symbol have more non-zero components. However, as mentioned in the text, the deformation energy over the disclination loop can not be calculated in the two-dimensional model. If a more detailed analysis is necessary for various nematic droplet shapes, three-dimensional analysis might be desirable.

Appendix A: Lattice generation

In a numerical analysis, the regions to be studied are covered by discrete lattices, and the information is given only on an individual lattice point. In many cases, the values in the inner region are given by the values on the boundaries to be analysed. Especially in the liquid crystal problem, the alignment on the boundaries seem to be decisive. Therefore, the discretization lattice should reflect the boundary structure as correctly as possible.

If the boundary values are given, a discretization lattice system can be generated by the solving equations [5], as a Dirichlet problem,

$$g^{ij}r_{\xi i\xi j}+P^{k}r_{\xi k}=0. \tag{A 1}$$

Here, ξ^{i} represents the ith lattice line and P^{k} controls the line shape, which is attracted or repulsed toward the particular line or point. The contravariant metric

tensor g^{ij} is given by equation (13). In the text, ξ^is constitute the curvilinear coordinates.

Two lattice systems have been made. One lattice system covers two electrodes, polymer material and nematic droplet surface. Another one corresponds to the inside of the droplet. These two lattice systems are coincident on the droplet surface. Discretization lattices including a spheroid are shown in figure 8, as an example.

Appendix B: Director distribution by Kilian and Hess's method

In this Appendix, the director distribution is numerically calculated by using Kilian and Hess's method on the curvilinear system. If equation (24) is multiplied by $\varepsilon_{pki}S^k_j$ and the resultant is contracted with respect to i, j and k, we get

$$\varepsilon_{pki}n^k h^i = (\mathbf{n}\times\mathbf{h})_p = 0. \tag{B 1}$$

Here, a molecular field h is

$$h^i = n_j\left(\Delta n^i n^j + \frac{1}{2}\varepsilon_a \overline{E^i E^j}\right). \tag{B 2}$$

Equation (B 1) states that the director should align parallel to the molecular field **h** [13]. Therefore, if the renormalization constant is denoted by λ, equation (B 1) is rewritten

$$n^i = \lambda h^i. \tag{B 3}$$

This equation determines the director distribution in a nematic droplet, if an appropriate boundary condition is given. It should be noticed that expression (B 3) is a non-linear equation, with respect to the director n^i. Generalized Poisson equations (26) and (27) ar used in its form, because the director is known.

The discretization is carried out before the contraction for j in equation (B 2). Discretizations for $\Delta n^i n^j$ have the same form as equation (33), if S^{ij} is replace by

The same distribution as in figure 3 (*a*) has been obtained in the absence of an external field for the spherical droplet, shown in figure 2 (*a*). If a high voltage is applied between the electrodes, the disclination ring sticks on the droplet surface. Even if the external field is set back to zero value, after such a high voltage

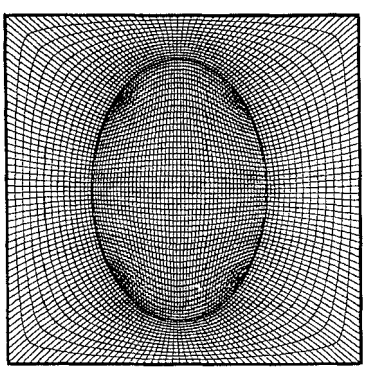

Figure 8. Discretizing lattice system. The thick lines represent lines on which coordinates are given as boundary values.

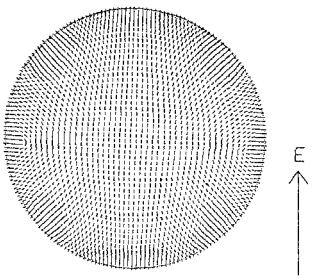

Figure 9. Director distribution, when an applied field is set back to zero value after a high field application.

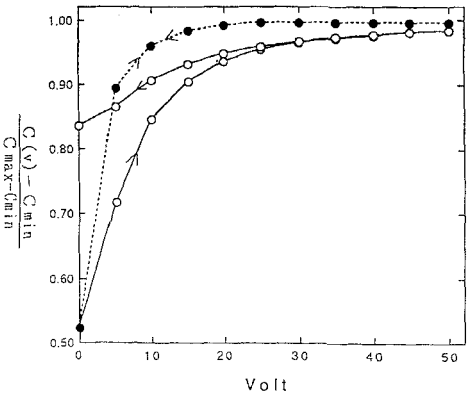

Figure 10. Differential electric capacity versus applied voltage characteristics for the spherical droplet. —○—, values for director distributions calculated by Kilian and Hess's method; – – – ● – – –, calculated by our method.

application, the same director distribution does not appear in this calculation. As shown in figure 9, the disclination ring continues to have a large radius, whose value is near that for the sphere.

Corresponding to these director distribution behaviours, the differential electric capacity has a large hysteresis in the voltage–capacity characteristics, as shown in figure 10.

References

[1] FERGASON, J., 1985, *SID, International Symposium Digest of Technical Papers*, **16,** 68.
[2] DOANE, J. W., 1990, *Liquid Crystals: Applications and Uses*, Vol. 1 edited by B. Bahadur (World Scientific Publishing Company), pp. 361–395.
[3] ONDRIS-CRAWFORD, R., BOYKO, E. P., WAGNER, B. G., ERDMANN, J. H., ZUMER, S., and DOANE, J. W., 1991, *J. appl. Phys.*, **69,** 6380.
[4] DE GENNES, P. G., 1971, *Molec. Crystals liq. Crystals*, **12,** 193.
[5] THOMPSON, J. F., WARSI, Z. U. A., and MASTIN, C. W., 1985, *Numerical Grid Generation* (North-Holland), p. 201.
[6] ZUMER, S., and DOANE, J. W., 1986, *Phys. Rev.* A, **34,** 3373.
[7] ZUMER, S., 1988, *Phys. Rev.* A, **37,** 4006.

[8] SHERMAN, R. D., 1989, *Phys. Rev.* A, **40,** 1591.
[9] KILIAN, A., and HESS, S., 1989, *Z. Naturf. (a)*, **44,** 693.
[10] KILIAN, A., 1993, *Liq. Crystals*, **14,** 1189.
[11] SCHOPOHL, N., and SLUCKIN, T. J., 1987, *Phys. Rev. Lett.*, **59,** 2582.
[12] GARTLAND JR., E. C., PALFFY-MUHORAY, P., and VARGA, R. S., 1991, *Molec. Crystals liq. Crystals*, **199,** 429.
[13] DE GENNES, P. G., 1974, *The Physics of Liquid Crystals* (Clarendon Press), p. 68.